
Equilibrium Residuals Expose Three Regimes of Matrix-Game Strategic Reasoning in Language Models

Wenhua Nie BINHAN LUO Zijie Meng
Jyh-Shing Roger Jang Ching-Wen Ma

Correspondence: Wenhua Nie, National Taiwan University
d13944014@ntu.edu.tw

Abstract

Large language models can score well on named game-theory benchmarks while failing on the same strategic computation once semantic cues are removed. We show this gap with procedurally generated zero-sum matrix games: a model that recognizes familiar games drops to 34%, 18%, and 2% success on anonymous 2×2 , 3×3 , and 5×5 payoff matrices. The benchmark separates semantic recall, learned approximate Nash computation, and an output-interface bottleneck that limits scale. Training only on 2×2 and 3×3 games, supervised fine-tuning raises unseen 5×5 – 7×7 success from 2% to 61%, while exploitability-reward training averages 37% with high seed variance. We prove that the exploitability residual is 2-Lipschitz in payoff perturbations, unlike discontinuous vertex-returning LP equilibrium selectors, explaining why residual training can transfer under payoff shifts even when formatting instability limits mean performance. A dominated-action padding experiment provides causal evidence: trained models solve 3×3 games embedded in much larger matrices, while random-padded controls fail and dense 12×12 games remain near failure. Procedural evaluation is therefore necessary for measuring strategic reasoning, and residual rewards expose a real but format-limited route to approximate equilibrium computation.

1 Introduction

Can large language models reason strategically in matrix games, or do they merely recall textbook solutions? Recent evaluations report that frontier LLMs, when given chain-of-thought prompting, select Nash-equilibrium actions in classic games such as the Prisoner’s Dilemma, Chicken, and Battle of the Sexes with high accuracy [Gandhi et al., 2023], fueling claims that language models possess genuine game-theoretic competence. Systematic analyses further probe LLM rationality in economic games, finding persistent gaps in formal strategic reasoning [Fan et al., 2024]. However, these benchmarks share a critical confound: every test instance is a *named* game whose equilibrium has appeared thousands of times in the training corpus.

We demonstrate that this apparent competence is fragile. When we strip away the semantic cues and present anonymous procedural payoff matrices, performance drops to 34%, 18%, and 2% on anonymous random 2×2 , 3×3 , and 5×5 matrices (Figure 1, left). Few-shot prompting with solved examples does not help—it actually *hurts*, reducing success from 34% to 10% on 2×2 games, suggesting that examples trigger template-matching rather than algorithmic reasoning.

This memorization–computation gap raises a fundamental question: *can LLMs learn to actually compute equilibria, rather than merely recall them?* We investigate this using procedurally generated

matrix games as a controlled microscope. Each training step presents a freshly sampled payoff matrix, eliminating the possibility of memorization. We study two learning paradigms:

- **SFT** (Supervised Fine-Tuning): the model is trained on solver-labeled (matrix, Nash strategy) pairs computed by linear programming.
- **VERGE** (Verifiable Equilibrium-Regret GRPO): the model receives only an exploitability reward—a scalar certificate measuring distance from Nash equilibrium—with no access to the equilibrium itself.

Both methods, trained exclusively on 2×2 and 3×3 games, produce models that generalize to unseen 5×5 – 7×7 games, improving success rates (exploitability < 0.10) from 2% to 61% (SFT) and 37% on average for VERGE (minimum seed 14%; higher variance but no solver labels needed). Our goal is not to claim that VERGE is the best in-distribution solver—SFT with oracle labels is stronger there—but to use the contrast between label imitation and residual rewards as a diagnostic for what kind of computation transfers. We therefore treat VERGE as a mechanism probe rather than a deployment-ready solver: the central evidence is the separation among semantic lookup, approximate computation, and output-interface failure. Both methods outperform the maximin pure-strategy heuristic at 5×5 (28%) and uniform mixing (4%).

A deeper analysis reveals three distinct regimes in this matrix-game setting, each governed by different mechanisms:

Regime I: Semantic Lookup. The base model retrieves memorized name→action mappings. This regime achieves perfect accuracy on textbook games but degrades sharply on procedural instances, and is disrupted rather than aided by few-shot examples.

Regime II: Learned Approximate Computation. Fine-tuned models exhibit genuine algorithmic behavior: they satisfy game-theoretic invariances (permutation equivariance error < 0.06 ; payoff shift/scale invariance error < 0.06) and generalize across game sizes. Under a near-OOD payoff-distribution shift (integer→Gaussian), a single VERGE checkpoint substantially outperforms SFT, but 100-game multi-seed replication shows that this transfer is seed- and format-sensitive rather than a stable mean advantage. This is consistent with our theoretical result that exploitability residuals are Lipschitz-stable in the payoff matrix while LP equilibrium selectors are discontinuous at support boundaries, but the theorem is only a mechanism probe, not a learned-policy generalization bound.

Regime III: Output-Interface Failure. Both methods exhibit a sharp performance cliff at $n \approx 12$. We provide evidence ruling out token length alone: 3×3 games padded to 12×12 token counts retain 83% success, while true 12×12 games achieve only 7%. Embedding 3×3 games into 12×12 matrices via iteratively dominated padding yields high success for trained models (SFT $95 \pm 8\%$ over three seeds; VERGE 90% in the diagnostic seed), while random-padded controls fail (Figure 1, right), leaving strategic depth and structured serialization as the remaining bottlenecks. A low-rank curriculum tradeoff reinforces this finding: training on larger games (3–5) improves conditional strategy quality but sharply degrades output-format generalization (valid rate at 12×12 drops from 99% to 0%).

We further prove (Theorem 1) that the exploitability residual is 2-Lipschitz in payoff perturbations, while vertex-returning LP equilibrium selectors are discontinuous. This theorem provides a mechanism consistent with the observed pattern: residual rewards can be more stable under payoff-distribution shift, while label imitation can still dominate when exact solver labels match the test distribution.

Contributions. Our main contributions are:

1. A causal audit showing that LLM game-theoretic competence on named matrix-game benchmarks reflects semantic recall, not computation, with procedural and invariance-based evidence (Section 3.1).
2. A controlled training comparison showing that solver-supervised SFT is stronger in-distribution, while residual-reward VERGE does not achieve a stable mean transfer advantage over SFT but can produce high-variance payoff-shift checkpoints (Sections 3.2 and 4.2).

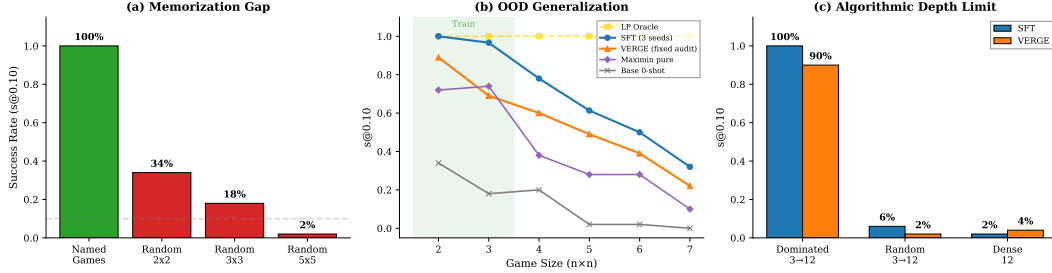


Figure 1: **Three regimes of matrix-game strategic reasoning in LLMs.** (a) Base model performs well on named games but falls to 34%, 18%, and 2% on random 2×2 , 3×3 , and 5×5 matrices (memorization gap). (b) SFT and VERGE trained on $2\text{--}3 \times 3$ generalize to 7×7 OOD, far exceeding maximin and base. (c) 3×3 games embedded in 12×12 matrices succeed for both SFT and VERGE, while dense and random-padded 12×12 games fail—a depth/serialization bottleneck in this setting rather than a token-length artifact.

- Controlled evidence ruling out token length alone as the explanation for the $n \approx 12$ cliff under our LoRA-adapted matrix-game setting, leaving strategic depth and serialization as the bottleneck candidates (Section 4.3).
- A formal gradient-cancellation result proving that role-merged GRPO in zero-sum self-play yields zero advantage-weighted strategic gradient, motivating the cooperative exploitability formulation (Section B).

2 Related Work

Strategic reasoning evaluation in LLMs. A growing body of work evaluates LLM behavior in strategic settings. Gandhi et al. [2023] show that chain-of-thought prompting enables LLMs to generalize strategic behavior across classic games; related prompting work shows that explicit reasoning traces can improve algorithmic tasks [Wei et al., 2022, Kojima et al., 2022, Nye et al., 2021, Zelikman et al., 2022]. Duan et al. [2024] introduce GTBench, showing that even frontier models fail on many game-theoretic tasks. Fan et al. [2024] study whether LLMs can serve as rational agents in economic games. Silva [2024] evaluate LLMs on mixed-strategy Nash games and find that performance degrades under even slight game modifications. TMGBench [Wang et al., 2024] improves coverage over 2×2 game types and story contexts, but remains an evaluation benchmark rather than a training and mechanistic analysis framework. Richer strategic agents such as Cicero combine language with planning in Diplomacy [Bakhtin et al., 2022]; our matrix setting is narrower but gives exact certificates. These works share a critical limitation: they primarily evaluate named or small structured games whose equilibria can leak through the training corpus. Our procedural-generation approach eliminates this confound by testing on freshly sampled payoff matrices, revealing that apparent strategic competence is largely memorization.

Algorithmic reasoning and length generalization in transformers. Transformers have been studied as computational devices that can learn algorithms from examples [Garg et al., 2022]. Work on length generalization shows that models trained on short sequences often fail on longer ones, with the failure mode depending on positional encoding and task structure [Anil et al., 2022]. Our dominated-padding experiment connects to this literature by separating two failure modes: output-length limitations (which we rule out) and algorithmic complexity (which remains as the bottleneck candidate at $n \approx 12$).

Equilibrium computation. Classical computational game theory studies Nash equilibria and algorithms for matrix games and beyond [Nash, 1951, Lemke and Jr., 1964, Nisan et al., 2007]. We use the zero-sum LP-solvable case because it gives exact exploitability certificates for evaluation.

Reinforcement learning from verifiable rewards. RLVR has emerged as an alternative to human preference learning, using mathematical verifiers [Shao et al., 2024], code execution [Le et al., 2022],

or formal proofs as reward signals. Our exploitability reward is a game-theoretic instance of this paradigm: it provides a scalar certificate of solution quality without revealing the solution itself, analogous in spirit to verifier-based reward modeling for math, step-level verification, and preference learning [Cobbe et al., 2021, Lightman et al., 2023, Christiano et al., 2017, Guo et al., 2025]. Our multi-seed replication shows verifier rewards can produce high-transfer checkpoints but not stable mean dominance, making exploitability a diagnostic rather than proof of RL superiority.

Self-play and multi-agent RL for LLMs. Self-play has been applied to LLMs for preference optimization [Wu et al., 2024], iterative fine-tuning [Chen et al., 2024], and general improvement [Yuan et al., 2024]. MARSHAL [Yuan et al., 2025] trains strategic LLM agents through multi-agent self-play in cooperative and competitive games, showing gains on held-out games and reasoning tasks. Munos et al. [2024] frame preference optimization as Nash equilibrium finding. In multi-agent RL, Policy-Space Response Oracles (PSRO) [Lanctot et al., 2017] provide a principled framework for computing Nash equilibria through iterative best-response computation. These works use “self-play” loosely—the model competes against itself for quality improvement, long-horizon interaction, or preference optimization. We study the classical matrix-game sense with exact exploitability certificates, and we prove an implementation-specific gradient-cancellation result (Section B) showing that role-merged GRPO normalization removes the advantage-weighted strategic gradient in this setting, motivating our cooperative exploitability formulation instead.

GRPO and policy gradient methods. GRPO [Shao et al., 2024] replaces the PPO critic with group-relative normalization, showing strong results on mathematical reasoning. It has since been widely adopted for LLM post-training. We prove that role-merged GRPO normalization in zero-sum self-play yields zero advantage-weighted strategic gradient (Section B), motivating our cooperative exploitability formulation where each response is independently scored.

3 Method and Theory

3.1 Procedural Game Testbed

We study two-player zero-sum matrix games defined by a payoff matrix $A \in \mathbb{R}^{n \times n}$, where the row player receives A_{ij} and the column player receives $-A_{ij}$ when row i and column j are played. A *mixed strategy* is a probability distribution over actions: $\mathbf{p} \in \Delta^n$ for the row player, $\mathbf{q} \in \Delta^n$ for the column player.

Definition 1 (Exploitability / NashConv). *For strategies (\mathbf{p}, \mathbf{q}) in a zero-sum game with payoff matrix A , the exploitability is:*

$$\text{Exploit}(A, \mathbf{p}, \mathbf{q}) = \underbrace{\max_i (A\mathbf{q})_i - \mathbf{p}^\top A\mathbf{q}}_{\text{row regret}} + \underbrace{\mathbf{p}^\top A\mathbf{q} - \min_j (\mathbf{p}^\top A)_j}_{\text{column regret}}. \quad (1)$$

Exploit = 0 if and only if (\mathbf{p}, \mathbf{q}) is a Nash equilibrium. We normalize by the payoff range: $\bar{\text{Exploit}} = \text{Exploit} / (2(\max A - \min A))$, and define the exploitability reward as $r = 1 - \bar{\text{Exploit}} \in [0, 1]$.¹

Game generation. Each training step samples a fresh $n \times n$ matrix with integer entries from $[-9, 9]$, normalized to $[-2, 2]$ by the payoff range. Training uses $n \in \{2, 3\}$; evaluation extends to $n \in \{2, \dots, 7\}$ (OOD) and $n \in \{8, \dots, 20\}$ (far OOD). This procedural generation eliminates memorization: the model must analyze each matrix from scratch.

Prompt and output format. The model receives the matrix in numerical form and outputs a JSON object `{"row": [...], "col": [...]}` specifying mixed strategies for both players. Strategies are normalized to the probability simplex after parsing.

Cooperative exploitability formulation. In both training methods (SFT and VERGE), the model proposes a complete strategy pair (\mathbf{p}, \mathbf{q}) per turn, receiving the exploitability reward $r = 1 - \bar{\text{Exploit}}(A, \mathbf{p}, \mathbf{q})$. This is a single-agent cooperative formulation: each response is scored independently on how close its proposed strategies are to a Nash equilibrium. We note that a natural

¹When $\max A = \min A$ (constant matrix), we perturb one entry by +1 to avoid division by zero; see Section C.

alternative—role-merged self-play where each response is scored as both row and column player—leads to gradient cancellation (Section B). Our cooperative formulation avoids this pathology by construction.

3.2 Two Teaching Methods

SFT (Supervised Fine-Tuning). For each generated game, we compute the Nash equilibrium using linear programming (the minimax theorem guarantees existence in zero-sum games). The model is trained with cross-entropy loss on (matrix, equilibrium) pairs, using LoRA ($r = 32$, $\alpha = 64$) on all attention and MLP projections.

VERGE (Verifiable Equilibrium-Regret GRPO). The model generates strategy proposals and receives the exploitability reward $r = 1 - \text{Exploit}$ as feedback. No Nash equilibrium labels are provided. GRPO [Shao et al., 2024] generates $G = 8$ samples per game and computes group-relative advantages over the accumulated training batch, with clipped policy gradient updates and KL regularization against the reference policy.

Theoretical comparison. SFT and VERGE optimize fundamentally different objectives. SFT imitates a specific equilibrium selector $T(A) = (\mathbf{p}^*, \mathbf{q}^*)$ determined by the LP solver. VERGE minimizes the exploitability residual $\text{Exploit}(A, \mathbf{p}, \mathbf{q})$. The following elementary design lemma characterizes their distinct stability properties and motivates the payoff-shift diagnostics; it is not a learned-policy generalization bound:

Theorem 1 (Residual stability vs. selector instability). *For any fixed strategies $(\mathbf{p}, \mathbf{q}) \in \Delta^n \times \Delta^n$:*

$$|\text{Exploit}(A, \mathbf{p}, \mathbf{q}) - \text{Exploit}(B, \mathbf{p}, \mathbf{q})| \leq 2\|A - B\|_\infty. \quad (2)$$

That is, $\text{Exploit}(\cdot, \mathbf{p}, \mathbf{q})$ is Lipschitz in the payoff matrix.

Conversely, for any $\delta > 0$, there exist games A, A' with $\|A - A'\|_\infty < \delta$ such that $\|T(A) - T(A')\|_1 = \Omega(1)$, where T is any equilibrium selector that returns a vertex solution at degeneracy (as common deterministic LP tie-breaking rules do).

Proof sketch. Expanding (1), the $\mathbf{p}^\top A \mathbf{q}$ terms cancel, giving $\text{Exploit}(A, \mathbf{p}, \mathbf{q}) = \max_i (A \mathbf{q})_i - \min_j (\mathbf{p}^\top A)_j$. The Lipschitz bound follows from $|\max_i (A \mathbf{q})_i - \max_i (B \mathbf{q})_i| \leq \|A - B\|_\infty$ (since $\|\mathbf{q}\|_1 = 1$) and the analogous bound for the \min_j term, where $\|A - B\|_\infty = \max_{i,j} |A_{ij} - B_{ij}|$ is the max-entry norm. Selector instability follows from degeneracy: for the scaled game $A_\epsilon = \epsilon \cdot M$ where M has a unique interior equilibrium, $T(A_\epsilon) \rightarrow T(M)$ as $\epsilon \rightarrow 0^+$, but at $\epsilon = 0$ the all-zeros matrix admits every strategy as a Nash equilibrium, and a vertex-returning tie breaker returns a vertex, causing an $\Omega(1)$ jump. Full proof in Section A. \square

Consequence. For any fixed strategy pair, VERGE’s verification signal is smooth under payoff perturbations, whereas a deterministic solver label can jump at support-boundary degeneracies. This does not prove learned-model OOD generalization; it motivates the selected payoff-shift tests in Section 4.2.

Why not zero-sum self-play? A natural alternative to cooperative exploitability training is competitive self-play, where each response is scored as both row and column player with antisymmetric rewards $(r_i, -r_i)$. We prove in Section B that *role-merged* GRPO—where the same generated output y_k is evaluated in both roles and both rewards enter the same normalization group—yields zero advantage-weighted strategic gradient, excluding any KL term that only pulls toward the reference policy. This specific failure mode motivates our cooperative exploitability formulation, where GRPO with sufficient gradient accumulation trains stably (see Section C for training details).

4 Experiments

All experiments use Qwen3.5-9B with LoRA ($r = 32$, $\alpha = 64$) on A800-80GB GPUs. SFT and VERGE train for 2000 steps with learning rates 5×10^{-5} and 10^{-5} . Evaluation uses 50 games per size and four samples per game at temperature 0.7. We report $s@0.10$: the fraction of games where the *best-of-4* sample achieves $\text{Exploit} < 0.10$. This uses oracle exploitability selection and

Table 1: OOD generalization on zero-sum games (train 2–3, test 2–7). All methods use the same evaluation games (seed=99, 50 games per size). $s@0.10$ is best-of-4 success with exploitability selection; pass@1 uses only the first sampled output. Fine-tuned rows report mean \pm std over 3 independent training seeds; dashes mark unevaluated few-shot sizes.

| Method | 2×2 | 3×3 | 4×4 | 5×5 | 6×6 | 7×7 |
|--------------------------|-----------------------|-----------------------|-----------------------|-----------------------|-----------------------|-----------------------|
| Base (0-shot) | 0.34 | 0.18 | 0.20 | 0.02 | 0.02 | 0.00 |
| Few-shot (3 ex.) | 0.10 | 0.02 | 0.00 | 0.00 | – | – |
| Qwen3-32B (8% valid) | 0.00 | 0.04 | 0.02 | 0.00 | 0.02 | 0.00 |
| Uniform | 0.18 | 0.04 | 0.16 | 0.04 | 0.08 | 0.04 |
| Maximin (pure) | 0.72 | 0.74 | 0.38 | 0.28 | 0.28 | 0.10 |
| SFT $s@0.10$ (3 seeds) | 1.00 \pm .00 | 0.97 \pm .04 | 0.78 \pm .00 | 0.61 \pm .09 | 0.50 \pm .05 | 0.32 \pm .09 |
| SFT pass@1 | 1.00 \pm .00 | 0.84 \pm .09 | 0.49 \pm .01 | 0.33 \pm .07 | 0.23 \pm .03 | 0.12 \pm .03 |
| Llama-3-8B SFT $s@0.10$ | – | – | – | 0.61 | – | 0.18 |
| Llama-3-8B SFT pass@1 | – | – | – | 0.36 | – | 0.07 |
| VERGE $s@0.10$ (3 seeds) | 0.85 \pm .12 | 0.66 \pm .22 | 0.50 \pm .24 | 0.37 \pm .22 | 0.29 \pm .26 | 0.18 \pm .09 |
| VERGE pass@1 | 0.77 \pm .21 | 0.50 \pm .26 | 0.31 \pm .20 | 0.21 \pm .18 | 0.11 \pm .10 | 0.07 \pm .03 |
| LP Oracle | 1.00 | 1.00 | 1.00 | 1.00 | 1.00 | 1.00 |

therefore measures the learned hypothesis space, not deployment-ready decoding; the main OOD table also reports pass@1. All evaluation games use seed 99. The uniform row in Table 1 calibrates a non-adaptive mixed-strategy null: 4% success at both 5×5 and 7×7. For $N=50$, the worst-case binomial standard error is 7.1 percentage points; the distribution-transfer table uses $N=30$ diagnostic games per condition (9.1 points).

Evidence package. The experiments ask whether 2×2–3×3 training transfers to larger anonymous games, whether residual rewards behave differently from solver labels under payoff shift, whether the $n\approx 12$ cliff is caused by length, dimension, or strategic depth, whether higher-rank adapters remove it, and whether zero-sum self-play needs the cooperative exploitability objective. The positive claims are restricted to these controlled settings; we do not claim that VERGE globally dominates SFT.

4.1 Out-of-Distribution Generalization

Table 1 shows the core result. Both SFT and VERGE improve upon the base model: 5×5 success rises from 2% (base) to 61% (SFT) and 37% (VERGE; seeds 58%, 40%, and 14%), versus 28% for maximin pure strategy. A 150-game replication at 5×5/7×7 gives SFT 0.63 \pm .01/0.28 \pm .05 and VERGE 0.42 \pm .18/0.16 \pm .15, confirming the OOD pattern while preserving VERGE’s higher seed sensitivity. Thus VERGE’s primary diagnostic signal is not absolute performance—where SFT with oracle labels dominates—but selected distribution transfer (Section 4.2) and the absence of solver supervision. Few-shot prompting *decreases* performance (34% \rightarrow 10% at 2×2), suggesting template-matching interference rather than induced computation. Under this strict JSON-only output contract, a zero-shot Qwen3-32B format-stress baseline obtains mean $s@0.10 = 0.01$ and valid-output rate 0.08 across 2–7; we therefore do not interpret it as an isolated test of reasoning capacity.

Without oracle selection, SFT pass@1 remains far above the base model: 0.33 \pm 0.07 at 5×5 and 0.12 \pm 0.03 at 7×7, versus 0.00 for the base model at both sizes. VERGE pass@1 is 0.21 \pm 0.18 at 5×5 and 0.07 \pm 0.03 at 7×7. Best-of-4 therefore strengthens the headline numbers, but the pass@1 rows show that the OOD signal does not rely solely on oracle selection.

4.2 Distribution Transfer

Table 2 reveals a clear but scoped pattern. The single-seed diagnostic contains high-transfer VERGE cells on Gaussian payoffs, but a 100-game replication changes the conclusion from “mean advantage” to “high-variance mechanism probe.” Across three training seeds, SFT is stable on Gaussian 8×8 and 10×10 (0.49 \pm .02, 0.44 \pm .08). Final VERGE is lower and much higher variance (0.36 \pm .29, 0.28 \pm .30). VERGE-600 over 4 partially overlapping seeds reaches 0.45 \pm .22/0.53 \pm .34 at 8×8/10×10, but the shared seeds move in opposite directions, so we treat this as checkpoint

Table 2: Single-seed diagnostic distribution transfer (train: integer $[-9, 9]$; test: Gaussian, sparse, integer). $s@0.10$ on 8×8 to 20×20 OOD games, 30 games per condition for this table. The 100-game Gaussian replication uses 3 seeds for SFT/final VERGE and 4 partially overlapping seeds for VERGE-600. The uniform baseline becomes dominant at $n \geq 12$ on Gaussian/sparse due to random-matrix concentration; the learned models’ advantage is at smaller, structured sizes.

| Distribution | Method | 8×8 | 10×10 | 12×12 | 15×15 | 20×20 |
|--------------|---------|--------------|----------------|----------------|----------------|----------------|
| Gaussian | Uniform | 0.33 | 0.47 | 0.63 | 0.93 | 1.00 |
| | SFT | 0.50 | 0.30 | 0.40 | 0.20 | 0.37 |
| | VERGE | 0.83 | 0.60 | 0.33 | 0.27 | 0.00 |
| Sparse | Uniform | 0.83 | 1.00 | 1.00 | 1.00 | 1.00 |
| | SFT | 1.00 | 0.97 | 0.80 | 0.70 | 0.37 |
| | VERGE | 1.00 | 0.93 | 0.63 | 0.47 | 0.07 |
| Integer | Uniform | 0.03 | 0.03 | 0.00 | 0.10 | 0.10 |
| | SFT | 0.10 | 0.07 | 0.00 | 0.00 | 0.00 |
| | VERGE | 0.23 | 0.07 | 0.03 | 0.00 | 0.00 |

variability rather than a controlled early-vs-late gain. Thus residual rewards can produce high-transfer checkpoints, but output-format stability controls whether that potential appears in the final policy.

Importantly, the uniform (maximin) baseline becomes increasingly competitive on Gaussian and sparse distributions at large n : it reaches $s@0.10 = 1.00$ on Gaussian 20×20 and sparse 12–20. This occurs because large random matrices concentrate toward games where uniform is near-optimal. The learned models’ advantage is confined to $n \leq 10$ –12, before random-matrix concentration makes uniform mixing near-optimal. We do not interpret the small non-monotonic changes within a row (e.g., SFT on Gaussian 15–20) as scaling laws under this 30-game diagnostic evaluation.

On sparse games at 8×8 , SFT and VERGE both reach $s@0.10 = 1.00$, but SFT’s sample-level valid-output rate remains higher (100% vs. 70%). At larger sparse sizes this format gap widens (70% vs. 2.5% valid at 20×20), so when the bottleneck is format reliability rather than strategy quality, supervised label training has an advantage. Thus VERGE’s transfer advantage should be read as conditional on producing parseable strategies, not as a claim that residual rewards solve the output-interface problem. Its 0.00 on Gaussian 20×20 is therefore primarily a format-validity failure (valid rate 0%), not evidence that a parseable VERGE strategy is exploitable in every such game. On integer payoffs (the training distribution), both learned methods and the uniform baseline perform poorly at $n \geq 12$, consistent with the depth/serialization bottleneck identified in Section 4.3.

4.3 The $n \approx 12$ Depth/Serialization Bottleneck

Both methods show a sharp performance cliff near $n = 12$. We design two controls to test whether this reflects algorithmic complexity or output-length limitations.

Padding control. We pad 3×3 game prompts with irrelevant system-note text to match the exact token count of 12×12 prompts (798 tokens). If the cliff were caused by token length or positional encoding degradation, padded 3×3 games should also fail.

Dominated-action padding with random-padding control. We embed 3×3 games into 12×12 matrices by adding actions that are irrelevant under iterated dominance. New rows have payoffs below the original minimum (strictly dominated for the row player). On the original row support, new columns have payoffs above the original maximum and are therefore dominated for the column player, who minimizes the row player’s payoff. The true Nash equilibrium is unchanged—only the matrix dimension increases. As a negative control, we also place the same 3×3 block in the top-left corner of an otherwise random $N \times N$ game. If success came from detecting a familiar sub-block or from output-format shortcuts, random padding should also succeed; if dominated-action reasoning is the operative mechanism, only dominated padding should preserve high success.

Table 3 provides the strongest controlled evidence in the paper. Across three SFT seeds, 3×3 games embedded in 12×12 matrices via iteratively dominated padding achieve $s@0.10 = 0.95 \pm .08$ and

Table 3: Single-seed controlled evidence for the $n \approx 12$ cliff under LoRA adaptation via dominated-action padding and a random-padding negative control. Entries report $s@0.10$ over 50 games with 4 samples per game. Dominated padding preserves the original 3×3 equilibrium; random padding embeds the same 3×3 block but changes the game.

| Model | Condition | 8×8 | 12×12 | 15×15 | 20×20 |
|-------|-----------------------------|-------------|-------------|-------------|-------------|
| Base | Dense random | 0.00 | 0.00 | 0.00 | 0.00 |
| | Dominated $3 \rightarrow N$ | 0.00 | 0.00 | 0.02 | 0.00 |
| | Random $3 \rightarrow N$ | 0.00 | 0.00 | 0.00 | 0.00 |
| SFT | Dense random | 0.16 | 0.02 | 0.02 | 0.02 |
| | Dominated $3 \rightarrow N$ | 1.00 | 1.00 | 0.98 | 0.98 |
| | Random $3 \rightarrow N$ | 0.22 | 0.06 | 0.02 | 0.04 |
| VERGE | Dense random | 0.36 | 0.04 | 0.02 | 0.04 |
| | Dominated $3 \rightarrow N$ | 0.94 | 0.90 | 0.90 | 0.76 |
| | Random $3 \rightarrow N$ | 0.22 | 0.02 | 0.02 | 0.02 |

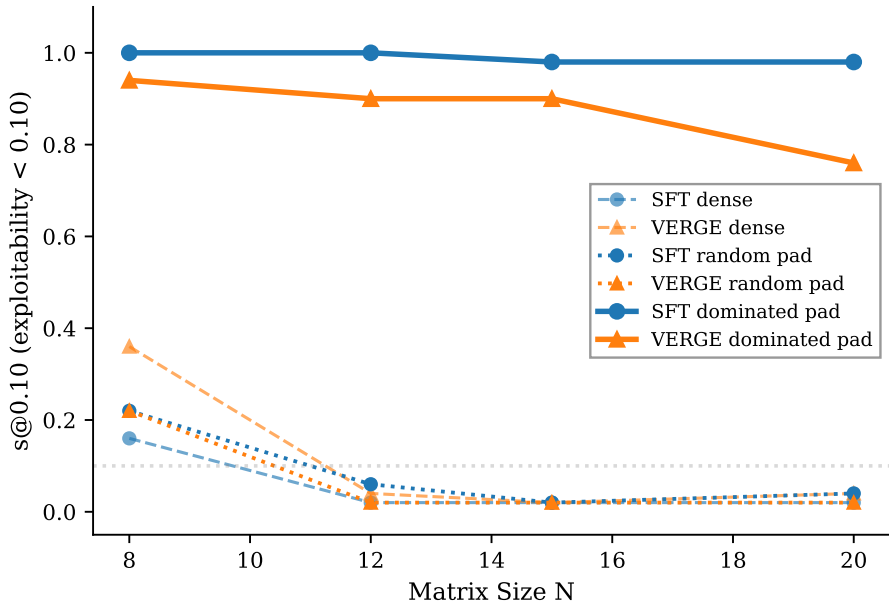


Figure 2: Dominated-padding experiment: $s@0.10$ as a function of padded matrix size N for $3 \times 3 \rightarrow N$ embeddings with iteratively dominated actions versus dense random $N \times N$ games and random-padded negative controls. Dominated embeddings remain far above both controls through $N=20$.

remain at 0.97 ± 0.01 even through 20×20 padding, while dense 12×12 games achieve 0.01 ± 0.01 and random-padded 12×12 games achieve only 0.06 in the negative-control seed. VERGE shows the same separation in the diagnostic seed: 0.90 on dominated $3 \rightarrow 12$ padding versus 0.04 on dense 12×12 and 0.02 on random $3 \rightarrow 12$ padding, with gradual degradation to 0.76 at 20×20 . The base model without fine-tuning fails on both dominated and random-padded games, confirming that dominated-action recognition requires training. The gap between dominated and random padding rules out token length and embedded-block recognition as sufficient explanations for success. Because the dominated and random controls have the same output dimensionality, the experiment also shows that output dimension alone is not sufficient to explain the success cases; the remaining failure on dense 12×12 games must involve strategic depth and structured serialization together.

Equivariance tests. To verify that the model learned genuine algorithmic behavior rather than position-dependent heuristics, we test game-theoretic invariances. For random row/column permutations of the payoff matrix, the mean reward difference is 0.019–0.054 (near-zero); for random payoff

shifts and positive scaling, the error is 0.029–0.044. The model is approximately equivariant to the symmetries that any game-solving algorithm must respect.

4.4 Curriculum and Serialization Tradeoff

Training on larger games ($n \in \{3, 4, 5\}$ instead of $\{2, 3\}$) reveals a surprising low-rank tradeoff. SFT-large averages $s@0.10 = 0.62$ at 7×7 over two seeds (vs. 0.32 for the three-seed SFT row on $\{2, 3\}$), showing improved *conditional* strategy quality. However, at 12×12 , the valid-output rate drops to 0% (compared to 99% for SFT on $\{2, 3\}$), meaning the model cannot produce a parseable probability vector of length 12.

Scratchpad-output supervision separates the two failure modes. In 700-step $r = 32$ controls with $N=30$ evaluation games, a 2–3 curriculum reaches only 0.19 ± 0.04 at 7×7 and 0.07 ± 0.06 at 12×12 . Expanding the curriculum to 2–5 improves near-OOD success to 0.50 ± 0.06 at 7×7 , but remains at 0.04 ± 0.04 at 12×12 despite high 12×12 valid-output rate (0.93 ± 0.05). Thus scratchpad supervision largely restores valid 12-dimensional serialization, but the resulting strategies remain exploitable.

This reveals two separable capabilities: *strategic computation* (selecting good probability weights) and *structured output emission* (serializing a valid n -dimensional distribution). A higher-rank control strengthens the diagnosis: increasing LoRA from $r = 32$ to $r = 128$ improves near-OOD success (final $s@0.10 = 1.00, 0.98, 0.80, 0.62, 0.42, 0.26$ on 2–7), but still yields 0% valid outputs and $s@0.10 = 0.00$ at 12×12 . The cliff is therefore not removed by scratchpad traces or a simple $4 \times$ LoRA-rank increase; whether full fine-tuning or explicit structured decoding resolves it remains open.

4.5 VERGE Training Dynamics

VERGE uses GRPO [Shao et al., 2024] with exploitability reward, $G = 8$ samples per generated game and batch-level advantage normalization with 4-step gradient accumulation. Training converges within 2000 steps on $2 \times 2/3 \times 3$ games. We note that gradient accumulation is critical: reducing to per-mini-batch updates (effective batch size 2) causes gradient norm spikes up to $93 \times$ baseline and training collapse within 500 steps (see Section C). This motivates our choice of $G = 8$ with 4-step accumulation throughout.

5 Discussion and Conclusion

Matrix games separate semantic lookup, learned approximate computation, and output-interface failure: procedural training improves random 5×5 success from 2% to 61%, while dominated-action padding isolates the $n \approx 12$ cliff from token length. The study is deliberately narrow—mostly Qwen3.5-9B LoRA on zero-sum matrices, with $N=30$ –150 controlled evaluations and seed-sensitive VERGE runs—so the three-regime claim should be read as a testbed result, not a universal claim about all strategic interaction. A scratchpad prompt alone remains near failure at 12×12 ($s@0.10 = 0.04$, $\text{pass}@1 = 0.00$), and scratchpad SFT improves 7×7 near-OOD success but leaves 12×12 success at 0.04 ± 0.04 . Full fine-tuning, structured decoding, variance-controlled residual RL, and general-sum or extensive-form games remain open.

References

- Cem Anil, Yuhuai Wu, Anders Andreassen, Aitor Lewkowycz, Vedant Misra, Vinay Ramasesh, Ambrose Slone, Guy Gur-Ari, Ethan Dyer, and Behnam Neyshabur. Exploring length generalization in large language models. In *NeurIPS*, 2022.
- Anton Bakhtin, Noam Brown, Emily Dinan, Gabriele Farina, Colin Flaherty, Daniel Fried, Andrew Goff, Jonathan Gray, Hengyuan Hu, Athul Paul Jacob, et al. Human-level play in the game of diplomacy by combining language models with strategic reasoning. *Science*, 2022.
- Zixiang Chen, Yihe Deng, Huizhuo Yuan, Kaixuan Ji, and Quanquan Gu. Self-play fine-tuning converts weak language models to strong language models. In *ICML*, 2024.
- Paul F. Christiano, Jan Leike, Tom B. Brown, Miljan Martic, Shane Legg, and Dario Amodei. Deep reinforcement learning from human preferences. In *NeurIPS*, 2017.
- Karl Cobbe, Vineet Kosaraju, Mohammad Bavarian, Mark Chen, Heewoo Jun, Lukasz Kaiser, Matthias Plappert, Jerry Tworek, Jacob Hilton, Reiichiro Nakano, Christopher Hesse, and John Schulman. Training verifiers to solve math word problems. *arXiv preprint arXiv:2110.14168*, 2021.
- Jinhao Duan, Renming Zhang, James Diffenderfer, Bhavya Kailkhura, Lichao Sun, Elias Stengel-Eskin, Mohit Bansal, Tianlong Chen, and Kaidi Xu. GTBench: Uncovering the strategic reasoning capabilities of LLMs via game-theoretic evaluations. In *NeurIPS*, 2024.
- Caoyun Fan, Jindou Chen, Yaohui Jin, and Hao He. Can large language models serve as rational players in game theory? A systematic analysis. In *AAAI*, 2024.
- Kanishk Gandhi, Dorsa Sadigh, and Noah D. Goodman. Strategic reasoning with language models. *arXiv preprint arXiv:2305.19165*, 2023.
- Shivam Garg, Dimitris Tsipras, Percy Liang, and Gregory Valiant. What can transformers learn in-context? A case study of simple function classes. In *NeurIPS*, 2022.
- Daya Guo, Dejian Yang, Haowei Zhang, Junxiao Song, Ruoyu Zhang, Runxin Xu, Qihao Zhu, Shirong Ma, Peiyi Wang, Xiao Bi, et al. DeepSeek-R1: Incentivizing reasoning capability in LLMs via reinforcement learning. *arXiv preprint arXiv:2501.12948*, 2025. doi: 10.48550/arXiv.2501.12948.
- Takeshi Kojima, Shixiang Shane Gu, Machel Reid, Yutaka Matsuo, and Yusuke Iwasawa. Large language models are zero-shot reasoners. In *NeurIPS*, 2022.
- Marc Lanctot, Vinicius Zambaldi, Audrunas Gruslys, Angeliki Lazaridou, Karl Tuyls, Julien Pérolat, David Silver, and Thore Graepel. A unified game-theoretic approach to multiagent reinforcement learning. In *NeurIPS*, 2017.
- Hung Le, Yue Wang, Akhilesh Deepak Gotmare, Silvio Savarese, and Steven Chu-Hong Hoi. Coderl: Mastering code generation through pretrained models and deep reinforcement learning. In *NeurIPS*, 2022.
- Carlton E. Lemke and Joseph T. Howson Jr. Equilibrium points of bimatrix games. *Journal of the Society for Industrial and Applied Mathematics*, 1964.
- Hunter Lightman, Vineet Kosaraju, Yuri Burda, Harrison Edwards, Bowen Baker, Teddy Lee, Jan Leike, John Schulman, Ilya Sutskever, and Karl Cobbe. Let’s verify step by step. *arXiv preprint arXiv:2305.20050*, 2023.
- Rémi Munos, Michal Valko, Daniele Calandriello, Mohammad Gheshlaghi Azar, Mark Rowland, Daniel Guo, Yunhao Tang, Matthieu Geist, Thomas Mesnard, et al. Nash learning from human feedback. In *ICML*, 2024.
- John Nash. Non-cooperative games. *Annals of Mathematics*, 1951.
- Noam Nisan, Tim Roughgarden, Éva Tardos, and Vijay V. Vazirani. *Algorithmic Game Theory*. Cambridge University Press, 2007.

Maxwell Nye, Anders Johan Andreassen, Guy Gur-Ari, Henryk Michalewski, Jacob Austin, David Bieber, David Dohan, Aitor Lewkowycz, Maarten Bosma, David Luan, Charles Sutton, and Augustus Odena. Show your work: Scratchpads for intermediate computation with language models. *arXiv preprint arXiv:2112.00114*, 2021.

Zhihong Shao, Peiyi Wang, Qihao Zhu, Runxin Xu, Junxiao Song, Xiao Bi, Haowei Zhang, Mingchuan Zhang, Y.K. Li, Y. Wu, and Daya Guo. DeepSeekMath: Pushing the limits of mathematical reasoning in open language models. *arXiv preprint arXiv:2402.03300*, 2024.

Alonso Silva. Large language models playing mixed strategy nash equilibrium games. *arXiv preprint arXiv:2406.10574*, 2024.

Haochuan Wang, Xiachong Feng, Lei Li, Zhanyue Qin, Dianbo Sui, and Lingpeng Kong. TMGBench: A systematic game benchmark for evaluating strategic reasoning abilities of LLMs. *arXiv preprint arXiv:2410.10479*, 2024.

Jason Wei, Xuezhi Wang, Dale Schuurmans, Maarten Bosma, Fei Xia, Ed Chi, Quoc V. Le, and Denny Zhou. Chain-of-thought prompting elicits reasoning in large language models. In *NeurIPS*, 2022.

Yue Wu, Zhiqing Sun, Huizhuo Yuan, Kaixuan Ji, Yiming Yang, and Quanquan Gu. Self-play preference optimization for language model alignment. In *NeurIPS*, 2024.

Huining Yuan, Zelai Xu, Zheyue Tan, Xiangmin Yi, Mo Guang, Kaiwen Long, Haojia Hui, Boxun Li, Xinlei Chen, Bo Zhao, Xiao-Ping Zhang, Chao Yu, and Yu Wang. MARSHAL: Incentivizing multi-agent reasoning via self-play with strategic LLMs. *arXiv preprint arXiv:2510.15414*, 2025.

Weizhe Yuan, Richard Yuanzhe Pang, Kyunghyun Cho, Xian Li, Sainbayar Sukhbaatar, Jing Xu, and Jason Weston. Self-rewarding language models. In *ICML*, 2024.

Eric Zelikman, Yuhuai Wu, Jesse Mu, and Noah D. Goodman. STaR: Bootstrapping reasoning with reasoning. In *NeurIPS*, 2022.

A Proof of Residual Stability (Theorem 1)

Proof. Fix $(\mathbf{p}, \mathbf{q}) \in \Delta^n \times \Delta^n$. For the row-regret term:

$$|\max_i (A\mathbf{q})_i - \max_i (B\mathbf{q})_i| \leq \max_i |(A\mathbf{q})_i - (B\mathbf{q})_i| \quad (3)$$

$$= \max_i |((A - B)\mathbf{q})_i| \quad (4)$$

$$\leq \max_i \sum_j |A_{ij} - B_{ij}| \cdot q_j \quad (5)$$

$$\leq \|A - B\|_\infty \cdot \|\mathbf{q}\|_1 = \|A - B\|_\infty. \quad (6)$$

Expanding (1), the $\mathbf{p}^\top A\mathbf{q}$ terms cancel: $\text{Exploit}(A, \mathbf{p}, \mathbf{q}) = \max_i (A\mathbf{q})_i - \min_j (\mathbf{p}^\top A)_j$. Thus:

$$\begin{aligned} & |\text{Exploit}(A, \mathbf{p}, \mathbf{q}) - \text{Exploit}(B, \mathbf{p}, \mathbf{q})| \\ & \leq |\max_i (A\mathbf{q})_i - \max_i (B\mathbf{q})_i| + |\min_j (\mathbf{p}^\top A)_j - \min_j (\mathbf{p}^\top B)_j| \end{aligned} \quad (7)$$

$$\leq \|A - B\|_\infty + \|A - B\|_\infty = 2\|A - B\|_\infty. \quad (8)$$

The second term follows by the same argument applied to the rows of $(A - B)^\top$ with $\|\mathbf{p}\|_1 = 1$. No dimension factor n appears because the simplex constraints absorb it.

For selector instability, let $M = \begin{pmatrix} 1 & -1 \\ -1 & 1 \end{pmatrix}$ (matching pennies) and consider the scaled family $A_\epsilon = \epsilon \cdot M$. For any $\epsilon > 0$, the unique Nash equilibrium is $\mathbf{p}^* = \mathbf{q}^* = (1/2, 1/2)$, so $T(A_\epsilon) = ((1/2, 1/2), (1/2, 1/2))$. At $\epsilon = 0$, the payoff matrix is all zeros, and every mixed strategy is a Nash equilibrium (exploitability is identically zero). Any vertex-returning selector (including common deterministic LP tie-breaking rules) returns a pure strategy, e.g. $T(A_0) = ((1, 0), (1, 0))$. Thus $\|T(A_\epsilon) - T(A_0)\|_1 \geq 1$ while $\|A_\epsilon - A_0\|_\infty = \epsilon \rightarrow 0$, confirming $\Omega(1)$ discontinuity for vertex-returning selectors. \square

B GRPO Gradient Cancellation in Zero-Sum Self-Play

This section proves that *role-merged* GRPO—where the same generated output is scored in both row and column roles within a single normalization group—yields exactly zero advantage-weighted strategic gradient. The statement excludes KL regularization, whose gradient can still pull the policy toward the reference but does not provide a game-theoretic learning signal. This is a specific failure mode of the naive implementation where one output serves both roles simultaneously; it does not apply to self-play architectures with separate policy copies or asymmetric normalization groups. The result motivates our use of cooperative exploitability rewards (Section 3.1).

Theorem 2 (GRPO gradient cancellation in symmetric zero-sum self-play). *Consider a zero-sum game where a shared policy π_θ plays both roles. GRPO generates G responses, each evaluated as both row (reward r_i) and column (reward $-r_i$). Under role-merged group normalization, the advantage-weighted policy-gradient component of GRPO is exactly $\mathbf{0}$ for every realization.*

Proof. Under symmetric zero-sum self-play, each game instance k produces a row reward r_k and a column reward $-r_k$. The group of $2G$ rewards is $\mathcal{R} = \{r_1, \dots, r_G, -r_1, \dots, -r_G\}$.

The group mean is $\bar{r} = \frac{1}{2G} \sum_{i=1}^G (r_i + (-r_i)) = 0$ identically (not in expectation—exactly zero for every realization).

The group standard deviation is $\sigma = \sqrt{\frac{1}{2G} \sum_{i=1}^G (r_i^2 + r_i^2)} = \sqrt{\frac{1}{G} \sum_{i=1}^G r_i^2}$. If $\sigma = 0$, then all $r_i = 0$ and all normalized advantages are zero, so the gradient is zero. Otherwise $\sigma > 0$ and the normalized advantages below are well-defined.

The advantage for the row-role response i is $\hat{A}_i^{\text{row}} = r_i/\sigma$, and for the column-role response i is $\hat{A}_i^{\text{col}} = -r_i/\sigma$. Since each response k proposes a complete strategy pair and is evaluated in both roles, the *same* output y_k appears in both gradient terms. The GRPO gradient contribution from response k is:

$$\hat{A}_k^{\text{row}} \nabla \log \pi_\theta(y_k) + \hat{A}_k^{\text{col}} \nabla \log \pi_\theta(y_k) = (\hat{A}_k^{\text{row}} + \hat{A}_k^{\text{col}}) \nabla \log \pi_\theta(y_k) = 0 \cdot \nabla \log \pi_\theta(y_k) = \mathbf{0}. \quad (9)$$

Summing over all G responses, the advantage-weighted strategic gradient is $\mathbf{0}$ —not in expectation, but exactly, for every realization. A KL regularization term, if included, is outside this cancellation statement and contributes only reference-policy pressure rather than a row/column strategic signal. \square

C Additional Experimental Details

LoRA configuration. All experiments use LoRA with $r = 32$, $\alpha = 64$, dropout 0.05, applied to $\{g, k, v, o, \text{gate, up, down}\}$ projections (7 target modules). Total trainable parameters: 58.2M / 9.0B (0.65%).

Optimizer and schedule. We use AdamW with weight decay 0.01, linear warmup followed by cosine decay, learning rates 5×10^{-5} for SFT and 1×10^{-5} for VERGE, and VERGE KL coefficient 0.05 with GRPO clipping range 0.2.

Game generation details. Integer payoffs are drawn uniformly from $\{-9, \dots, 9\}$, then normalized: $A \leftarrow 2A / (\max A - \min A)$, yielding entries in approximately $[-2, 2]$. If all entries are equal, one is perturbed by +1 to ensure non-degeneracy.

Evaluation protocol. For each game size n and evaluation set (fixed seed=99):

- Generate 50 random games (30 for intermediate checkpoints)
- For each game, generate 4 samples at temperature 0.7
- Parse JSON output; normalize to probability simplex
- Report best-of-4 exploitability reward and first-sample pass@1
- $s@0.10$ = fraction of games where best reward > 0.90

Computational cost. Per training seed, VERGE 2000 steps takes ~ 14 hours on $1 \times A800$, and SFT 2000 steps takes ~ 4 hours on $1 \times A800$. We parallelize independent seeds and evaluation jobs across available A800 GPUs. Full evaluation suite: ~ 2 hours per checkpoint.

D Limitations

This study is intentionally narrow. The main experiments use procedurally generated two-player zero-sum matrix games, mostly Qwen3.5-9B with LoRA adaptation, and fixed-size random evaluation sets rather than human or real-world strategic tasks. Cross-architecture evidence is limited, full fine-tuning is not evaluated, and the structured-output interface is left to the model rather than enforced by constrained decoding. VERGE should therefore be read as a residual-reward diagnostic rather than a stable method that dominates solver supervision. The conclusions identify controlled failure modes in this testbed; they do not establish a universal law of strategic reasoning across model families, game classes, or deployment settings.

E Broader Impact

This work is a synthetic evaluation and training study, not a deployed strategic agent. Positive impacts include sharper tests for whether language models reason procedurally or retrieve memorized solutions, which can improve evaluation practice for planning and decision-support systems. Negative impacts are possible if stronger strategic-reasoning agents are used in automated negotiation, persuasion, or planning settings without oversight. To limit release risk, the supplemental material provides code and synthetic game generators rather than trained agent checkpoints or a user-facing decision system.